Journal of the Korean Society of Oceanography
Vol. 35, No. 2, pp. 78—88 June 2000

Variational Approaches to Short Waves in Weakly Viscous Fluids

NAM-CHUL KIM
Research Institute of Oceanography, Seoul National University, Seoul 151-742, Korea

A weakly viscous wave and an approximate variational principle in viscous fluids are introduced, with which we can interpret the fundamentals such as how viscosity dissipation occurs with time elapse, and how the free surface boundary layer exists at the wavy surface in weakly viscous fluids. As an application, responses of a spherical buoy on the weakly viscous capillary gravity wave are investigated to show the viscosity effects. At the end, surfactant problems are briefly reviewed with the view of short viscous waves as expected future applications.

INTRODUCTION

Variational formulation is now popular and powerful in various fields where it is applicable. Variational approaches to wave dynamics have been issued actively since early sixties by many authors like Whitham (1974). Since then, many aspects involved in wave phenomena are still investigated by employing the methods based on variational calculus, not to mention specific examples. The discussion here reviews and describes what the variational principles are regarding force equilibrium equations, and how the specific variational principles work in basic wave types such as gravity waves, capillary-gravity waves, and a weakly viscous wave derived in the following sections. Equi-partitioning of kinetic & potential energies in capillary-gravity waves is also briefly discussed by inspecting the role of surface tension in potential energy. As an approximation of viscous waves, a weakly viscous wave type, equation (27), corresponding to its variational principle is introduced. With the help of this new wave, we can understand the fundamentals such as how viscosity dissipation occurs with time elapse, how rotational flows work to produce vorticity, and how the free surface boundary layer (FSBL) exists at wavy surfaces in weakly viscous fluids. The equi-partitioning between energies also applies in this weakly viscous wave, as it does in inviscid waves, in the sense of perturbation.

In the second half, responses of a spherical floating object on the weakly viscous capillary gravity wave are investigated as a specific application. The actual distributions of the viscous shear forces due to the free surface boundary layer flows are found across the intersection of the wave and the buoy at each time step employing a multiple coordinate system. This coordinate system consists of two sets of coordinates, one of which is a Cartesian system fixed in space, mainly for the representation of the wave, and the other is a spherical system moving with the spherical buoy. The simultaneous usage of multiple coordinate systems turns out an efficient and promising tool when we deal with multiple objects with different orientations as we did with the present wave-buoy problem. Wave forces are calculated by integrating the stresses numerically over the domain of the instant intersections. At the end, surfactants and its related problems are reviewed and discussed with the views of short waves, viscosity, varying surface tension, and remote sensing of ocean surfaces, each of which requires small scale, detailed and advanced information indispensable for the better understanding of global oceanic environments of the Earth.

*Corresponding author: nkim@ocean.snu.ac.kr

CAPILLARY-GRAVITY WAVES

Variational principle

The force equilibrium equation (Navier-Stokes Equation) is

$$\sum f_i = \frac{\partial \vec{V}}{\partial t} + \vec{V} \cdot \nabla \vec{V} + \frac{1}{\rho} \nabla P - \nu \nabla^2 \vec{V} + g\vec{k} = 0 \qquad (1)$$

where $\vec{V}$ is the fluid velocity vector, P is the fluid pressure, ν is the viscosity of fluid, ρ is the water density, and g is the gravity constant. For irrotational

flows in inviscid fluids, we can employ a scalar function to represent the velocity as below,

$$\sum f_i = \frac{\partial \vec{V}}{\partial t} + \vec{V}\cdot\nabla\vec{V} + \frac{1}{\rho}\nabla P + g\vec{k} = 0, \;\&\quad \vec{V} = \nabla\Phi \tag{2}$$

where Φ is the velocity potential representing irrotational flows.

-Virtual works by f_i

A virtual displacement in two dimensional flows is below by definition,

$$\delta\vec{s} = \delta x\vec{i} + \delta z\vec{k} \tag{3}$$

where (x, z) and $(\vec{i}, \vec{k})$ are the horizontal and vertical coordinates and their unit basis vectors in Cartesian coordinates. Then, the whole virtual work by the forces in the Navier-Stokes equation is defined as

$$\delta W_{NS} = \sum f_i \cdot \delta\vec{s} \tag{4}$$

or, for a control volume, the virtual work becomes

$$\delta W_{NS} = \iint_{xz}\left(\frac{\partial \vec{V}}{\partial t} + \vec{V}\cdot\nabla\vec{V} + \frac{1}{\rho}\nabla P + g\vec{k}\right)\cdot\delta\vec{s}\,dz\,dx$$

$$= \iint_{xz}\left(\nabla\left(\frac{\partial\Phi}{\partial t}\right) + \nabla\Phi\cdot\nabla(\nabla\Phi) + \frac{1}{\rho}\nabla P + g\vec{k}\right)\cdot\delta\vec{s}\,dz\,dx \tag{5}$$

or, with the help of variational calculus, we can get

$$\delta W_{NS} = \delta\left(\iint_{xz}\left(\nabla\frac{\partial\Phi}{\partial t} + \frac{1}{2}\nabla\Phi\cdot\nabla\Phi + \frac{1}{\rho}P + gz\right)dz\,dx\right) \tag{6}$$

-Virtual work by σ

Surface tension(σ) is usually assumed constant in the flows with free surfaces, then, the virtual displacement for surface tension is defined as

$$\delta\vec{s} = \delta x\vec{i} + \delta z\vec{k}\Big|_{\text{at surface}} = \delta s\vec{t} \tag{7}$$

where $\vec{t}$ is the unit tangential vector at the surface. Then, the virtual work (δW_σ) by the surface tension becomes

$$\delta W_\sigma = \sigma\vec{t}\cdot\delta s\vec{t} = \delta(\sigma s) \tag{8}$$

Since, at the surface, the arc-length of a wave profile is determined using the surface elevation as below

$$s = \int_x \sqrt{1+\zeta_{,x}^2}\,dx \tag{9}$$

where ζ is the surface elevation of the wave. Then, the virtual work due to the surface tension finally becomes

$$\delta W_\sigma = \delta\left(\sigma\int_x \sqrt{1+\zeta_{,x}^2}\,dx\right) \tag{10}$$

Therefore, the total virtual work in the capillary-gravity wave type is the sum of above two portions.

$$\delta W_{CG} = \delta W_{NS} + \delta W_\sigma \tag{11}$$

Or, the variational principle of the capillary-gravity wave type, which is nonlinear, becomes

$$\delta\left(\int_t\int_x\left(\int_z\left(\frac{\partial\Phi}{\partial t} + \frac{1}{2}\nabla\Phi\cdot\nabla\Phi + \frac{1}{\rho}P + gz\right)dz + \frac{\sigma}{\rho}\sqrt{1+\zeta_{,x}^2}\right)dx\right)dt = 0 \tag{12}$$

A variational principle and its associated equation set

For capillary-gravity waves in deep sea, the variational principle becomes equation (13) after trivial modifications,

$$\delta\left(\int_t\int_{x_f}^{x_l}\left(\int_{-\infty}^{\zeta}\left(\frac{\partial\Phi}{\partial t} + \frac{1}{2}\nabla\Phi\cdot\nabla\Phi + \frac{1}{\rho}P + gz\right)dz + \frac{\sigma}{\rho}\sqrt{1+\zeta_{,x}^2}\right)dx\right)dt = 0 \tag{13}$$

Variation with respect to Φ, and ζ leads us to the following equation set in equation (14)*. Since $\delta\Phi$ and $\Delta\zeta$ are arbitrary, each integrand in the equation (14) becomes zero, which results in a group of separated equations having those meanings at the right side.

$$\delta\tilde{W}_{CG} = \int_t\int_{x_f}^{x_l}\left(\frac{\partial}{\partial t}\int_{-\infty}^{\zeta}\delta\Phi\,dz + \frac{\partial}{\partial x}\int_{-\infty}^{\zeta}\Phi_{,x}\delta\Phi\,dz\right)dx\,dt$$

: conservation law

$$-\int_t\int_{x_f}^{x_l}\int_{-\infty}^{\zeta}(\Phi_{,xx}+\Phi_{,zz})\delta\Phi\,dz\,dx\,dt$$

: governing equation

$$+\int_t\int_{x_f}^{x_l}(\Phi_{,z}-\zeta_{,t}-\Phi_{,x}\zeta_{,x})\big|_{z=\zeta}\delta\Phi\,dx\,dt$$

: kinematic surface B. C.

$$+\int_t\int_{x_f}^{x_l}\left.\begin{pmatrix}\Phi_{,t}+\frac{1}{2}\nabla\Phi\cdot\nabla\Phi+\frac{P}{\rho}+gz\\ \left(-\frac{\sigma}{\rho}\right)\frac{1}{1+\zeta_{,x}^2}\left(\zeta_{,xx}\sqrt{1+\zeta_{,x}^2}-\frac{\zeta_{,x}^2}{\sqrt{1+\zeta_{,x}^2}}\right)\end{pmatrix}\right|_{z=\zeta}\delta\zeta\,dx\,dt$$

: dynamic surface B.C.

$$+\int_t\int_{x_f}^{x_l}\Phi_{,z}\big|_{z=-\infty}\delta\Phi\,dx\,dt \quad : \text{bottom B.C.}$$

*G.B. Whithams, Liner and nonlinear waves, John Wiley, New York, 1974.

$$+\int_t \frac{\zeta_{,x}}{\sqrt{1+\zeta_{,x}^2}}\Bigg|_{x_l,z=\zeta}^{x_r,z=\zeta}\delta\zeta \qquad \text{: corner condition}$$

$$=0 \tag{14}$$

The obtained equations, which are nonlinear, constitute a set of a governing equation with its boundary conditions representing the wave motions at the surfaces. With additional assumptions of linearization, the equations reduce to the ordinary linear wave equation set.

- Equi-partitioning of energies in capillary-gravity waves

kinetic energy stored in one wavelength is, after the assumption of linear wave profile, easily obtained using its definition as

$$E_k = \frac{1}{4}a^2\lambda(\rho g+\sigma k^2) \tag{15}$$

where a is the wave amplitude, λ is the wave length, and k is the wave number.

Potential energy in C-G waves consists of two works by gravity and by surface tension, therefore, the potential energy stored in one wavelength becomes

$$E_p = \int_0^\lambda\int_0^\zeta \rho z dz dx\cdot g+\int_0^\lambda \sigma\cdot(\sqrt{1+\zeta_{,x}^2}-1)dx \tag{16}$$

Just as the two energies balance each other in gravity waves, kinetic energy in capillary-gravity waves balances with the works by the two forces, the gravity and the surface tension, or $E_k = E_p$.

A WEAKLY VISCOUS WAVE (AN APPROXIMATION OF REAL WATER WAVES)

An approximate variational principle in weakly viscous fluids

If we employ an assumption on the velocity as below,

$$\vec{V} = \nabla\Phi+\nabla\times\vec{\tilde{\Psi}} = \nabla\times\vec{\Psi}+\nabla\times\vec{\tilde{\Psi}} \tag{17}$$

where $\vec{\Psi}$, and $\vec{\tilde{\Psi}}$ are stream functions for irrotational and rotational flows respectively in two dimensional (x, z) directions. Then, the weak viscosity guarantees that the irrotational portion turns out much greater than the rotational portion, which we can confirm later in equation (27), in other words,

$$|\nabla\Phi| = \left|\nabla\times\vec{\Psi}\right| \gg \left|\nabla\times\vec{\tilde{\Psi}}\right| \tag{18}$$

Virtual works in weakly viscous fluids are defined by the forces in the Navier-Stokes equations and the corresponding virtual displacement as follows.

$$\delta W = \sum f_i\cdot\delta\vec{s}, \tag{19}$$

where, $\sum f_i = \frac{\partial\vec{V}}{\partial t}+\vec{V}\cdot\nabla\vec{V}+\frac{1}{\rho}\nabla P-\nu\nabla^2\vec{V}+g\vec{k}$.

Then, the virtual work for a control volume can be expressed as

$$\begin{aligned}\delta W_{NS} &= \iint_{x\,z}\left(\frac{\partial\vec{V}}{\partial t}+\vec{V}\cdot\nabla\vec{V}+\frac{1}{\rho}\nabla P-\nu\nabla^2\vec{V}+g\vec{k}\right)\cdot\delta\vec{s}dzdx\\ &= \iint_{x\,z}\left(\frac{\partial}{\partial t}\left(\nabla\Phi+\nabla\times\vec{\tilde{\Psi}}\right)+\left(\nabla\Phi+\nabla\times\vec{\tilde{\Psi}}\right)\cdot\nabla\left(\nabla\Phi+\nabla\times\vec{\tilde{\Psi}}\right)\right.\\ &\quad\left.+\frac{1}{\rho}\nabla P-\nu\nabla^2\left(\nabla\Phi+\nabla\times\vec{\tilde{\Psi}}\right)+g\vec{k}\right)\cdot\delta\vec{s}dzdx\end{aligned} \tag{20}$$

After a series of variational manipulations, we can approximate the above virtual work as

$$\begin{aligned}\delta W_{NS} = \delta\Bigg(\iint_{x\,z}\Bigg(&\Phi_{,t}+\left(\frac{1}{2}(\Phi_{,x}-\tilde{\Psi}_{,z})^2+(\Phi_{,z}+\tilde{\Psi}_{,x})^2\right)\\ &|-\frac{1}{\nu}\tilde{\Psi}_{,t}(\Psi+\tilde{\Psi})+\frac{1}{\rho}P+gz\Bigg)dzdx\Bigg),\end{aligned} \tag{21}$$

since,

$$\delta(\tilde{\Psi}_{,t}(\Psi+\tilde{\Psi})) = \delta\tilde{\Psi}_{,t}(\Psi+\tilde{\Psi})+\tilde{\Psi}_{,t}\delta(\Psi+\tilde{\Psi})\cong\tilde{\Psi}_{,t}\delta(\Psi+\tilde{\Psi}) \tag{22}$$

The virtual work by the surface tension is assumed same as that in ordinary capillary gravity waves. Therefore, the variational principle for this weakly viscous wave type, which is genuinely nonlinear, can be approximated as below in equation (23) by employing the fact that rotational portion is smaller than others by one order with respect to the small viscosity ν.

$$\delta\left(\iint_{t\,x}\left(\int_{-\infty}^{\zeta}\left(\begin{array}{c}\Phi_{,t}+\frac{1}{2}\left\{\left(\nabla\Phi+\nabla\times\vec{\tilde{\Psi}}\right)\left(\nabla\Phi+\nabla\times\vec{\tilde{\Psi}}\right)\right\}\\ -\frac{1}{\nu}\tilde{\Psi}_{,t}(\Psi+\tilde{\Psi})+P+gz\\ +\frac{\sigma}{\rho}(1+\zeta_{,x}^2)^{1/2}\end{array}\right)dz\right)dxdt\right) = 0 \tag{23}$$

A free surface wave in weakly viscous fluids

With the same assumption on velocity in the previous section,

$$\vec{V} = \nabla\Phi+\nabla\times\vec{\tilde{\Psi}} = \nabla\times\vec{\Psi}+\nabla\times\vec{\tilde{\Psi}} \text{ with}$$

$$|\nabla\Phi| = \left|\nabla\times\vec{\Psi}\right| \gg \left|\nabla\times\vec{\tilde{\Psi}}\right|$$

and adding the assumption of linearization, we can get a governing equation set from the Navier-Stokes equation,

$$\nabla^2\Phi = 0, \quad \nabla^2\tilde{\Psi} = \frac{1}{\nu}\tilde{\Psi}_{,t} \tag{24}$$

and viscous boundary conditions as below.*

at surface

$$\zeta_{,t} = w, \ \& \ \Phi_{,t} + g\zeta = \left(-\frac{p}{\rho}\right) \ t>0 \tag{25}$$

$$\tau_{xz} \equiv \mu(u_{,z} + w_{,x}) = 0, \quad \tau_{zz} = 2\mu w_{,z} - p - \sigma\zeta_{,xx} = 0$$

at bottom

$$w = 0 \tag{26}$$

where u, w are horizontal and vertical fluid velocities respectively, and τ_{xz}, τ_{zz} are tangential and normal stresses on the free surface. If we solve the above equation set with proper approximations in the solution procedures by ignoring terms smaller than $O(\nu)$, we can get the below weakly viscous wave as an approximation of real water waves.

$$\zeta = \frac{a}{2}e^{-2\nu k^2 t}(e^{i(kx-\omega_0 t)} + \text{c.c.})$$

$$\Phi = \frac{a}{2}\left(\frac{\omega_o}{k}\right)e^{kz}e^{-2\nu k^2 t}\left(e^{i\left(kx-\omega_0 t-\frac{\pi}{2}\right)} + \text{c.c.}\right), \quad \Psi = -i\Phi$$

$$\tilde{\Psi} = \frac{a}{R_n}\left(\frac{\omega_o}{k}\right)e^{k\sqrt{\frac{R_n}{2}}z}e^{-2\nu k^2 t}\left(e^{i\left(-k\sqrt{\frac{R_n}{2}}z+kx-\omega_0 t+\frac{\pi}{2}\right)} + \text{c.c.}\right) = O(\nu) \tag{27abc}$$

where, $R_n = \dfrac{\omega_o}{\nu k^2} \gg 1$

For large Reynolds numbers, it is possible to describe the wave motions in weakly viscous fluids as shown in equation (27), and also simplify the dispersion equation which shows how the viscosity works separately as well as the frequency-wavelength relation in the derivation. The solution (27) states that every physical term undergoes dissipation due to the viscosity as time goes, and that the rate of dissipation relates with viscosity and wavenumber as much as $\exp(-2\nu k^2 t)$. Wave profiles are same as those of inviscid waves except the dissipation. They oscillate and propagate in the same fashion as a ordinary capillary-gravity wave does. There exists a rotational flow expressed in the stream-function which says, as an approximation, that it will oscillate in both directions horizontally as slow as irrotational flows and vertically as fast as square root of Reynolds number, and that the amplitude or the amount is so small as the order of the reciprocal of Reynolds number or $O(\nu)$, and that it will die out as it deepens as fast as $\exp(k\sqrt{R_n/2}\cdot z)$, while others decrease as fast as $\exp(kz)$. In other words, there exists a thin layer beneath the surface, where both irrotational flows and smaller rotational flows work, and outside of which flows become inviscid, and the thickness of which relates with wavenumber and Reynolds number in real waters as weakly viscous fluid.

Vorticity intensity and free surface boundary layer thickness

It is well known that there exists vorticity even in inviscid flows near free surfaces in order to satisfy the free surface boundary conditions. The vorticity existing in this wave type is as follows.

Vorticity intensity:

$$\begin{aligned} 2\Omega &= \nabla\times\vec{V} \\ &= O(2ka\omega_0) + O(\nu 2k^3 a) \end{aligned} \tag{28}$$

where $\vec{V} = \nabla\Phi + \nabla\times\vec{\tilde{\Psi}}$ as described in the equations (17) and (27bc).

Equation (28) says that in the weakly viscous flows with free surfaces, there exist two vorticity components, one of which is free from viscosity and the other is directly due to viscosity. The viscosity free vorticity which is also mentioned Longuet-Higgins [1992]*, becomes much bigger than the other portion under the assumption of weak viscosity contrary to the ordinary expectation. The vorticity also dissipates as fast as $\exp(-2\nu k^2 t)$ as time passes, and exists only within where the rotational stream function exists. The vorticity intensity at $z = -\delta_t$ reduces to 36% of that at surface where $\delta_t = (2\nu/\omega_o)^{1/2}$, and becomes 1.8% at $z = -4\delta_t$, which means that outside $4\delta_t$, irrotational motion dominates the fluid flows. It can be said that boundary layer thickness is order of $(2\nu/\omega_o)^{1/2}$, which coincides with the already known result before.

Energies dissipate as time passes in viscous fluids. In the case of above weakly viscous waves, the energy stored in a wavelength undergoes dissipation as fast as $\exp(-4\nu k^2 t)$ as shown in equation (29) since energy is proportional to the square of wave-height which dissipate at the rate of $\exp(-2\nu k^2 t)$. The energy in rotational flow portion is as small as $O(R_n^{-3/2})$ that becomes trivial in the present perturbation scale of

*J.W. Miles, Capillary-viscous forcing of surface waves, J. Fluid Mech. Vol. 219 1990.

*M.S. Longuet-Higgins, "Capillary rollers and bores", J. Fluid. Mech. Vol. 240, 1992.

$O(R_n^{-1})$.

$$E_p = \frac{1}{4}a^2\lambda(\rho g+\sigma k^2)\cdot e^{-4\nu k^2 t} \tag{29a}$$

$$E_k = \frac{1}{4}\rho a^2\lambda\frac{a_o^2}{k}\left(1+2\left(\frac{2}{R_n^3}\right)^{1/2}+2\left(\frac{2}{R_n^5}\right)^{1/2}\right)\cdot e^{-4\nu k^2 t} \tag{29b}$$

where $\alpha = \alpha_0+\nu\alpha_1+O(\nu^2)$, $\alpha_o^2 = \frac{\sigma k^3}{\rho}+gk$, $\alpha_1 = -2k$.

This weakly viscous wave is derived using perturbation technique with respect to the small number ν, in which sense the equi-partitioning between potential energy and kinetic energy also applies here as it does in inviscid waves.

APPLICATIONS

A spherical buoy on a weakly viscous capillary gravity wave

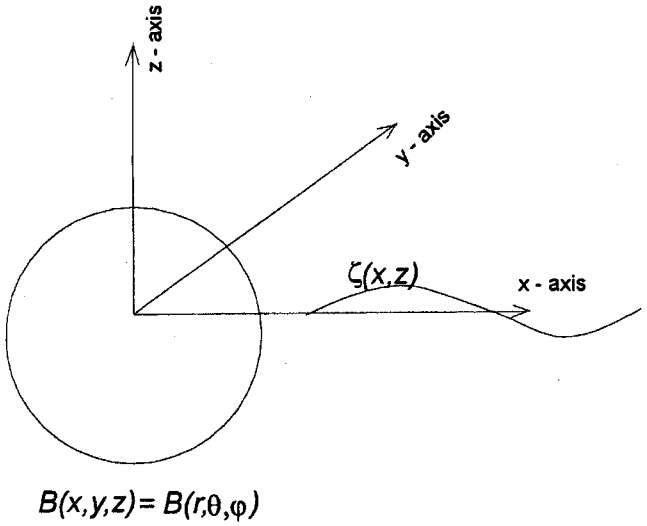

Fig. 1. A sperical buoy on a weakly viscous wave.

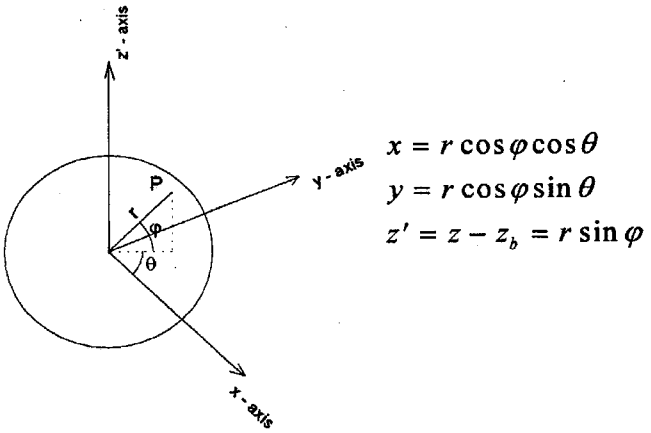

Fig. 2. Relationships between coordinate systems.

Coordinate systems involved

To describe the present problem effectively, two types of coordinate systems are used, one of which is a Cartesian system (x, y, z) fixed in space and the other is a spherical system (r, φ, θ) that is fixed at the buoy geometric center, i.e. moving with it.

Both coordinate systems are used simultaneously during the detailed calculations through numerical computations. The relationships between these two systems are as above. The z' is an intermediate variable meaning the vertical displacement of the buoy center from the horizontal x axis of the fixed coordinate system.

The instant intersection between the spherical buoy and the wave in motion

The waves can be described efficiently with respect to the fixed Cartesian coordinates (x, y, z) where y - axis is a dummy direction, and the geometry of the spherical buoy can be described in the both coordinate systems, however; when we consider the wave forces acting on the moving sphere, the spherical coordinates fixed at the buoy geometric center works better for the purpose, because we need normal and shear stresses acting on the three dimensional instant intersection between the buoy and the wave.

$$Z(x,z,t) = \frac{a}{2}e^{-2\nu k^2 t}(e^{i(kx-w_0 t)}+\text{c.c.}) \tag{30}$$

$$B(x,y,z,t) = r^2-(x^2+y^2+(z-z_b(t))^2) = 0 \tag{31}$$

$$\cos^2\varphi = \frac{x^2+y^2}{x^2+y^2+(\zeta-z_b)^2} \tag{32}$$

$$\tan\theta = \frac{y}{x} \tag{33}$$

where

$-r\le x\le r$, $-r\le y\le r$, $-r+z_b\le z\le r+z_b$, and

z_b = the location of the buoy center at $t = t_i$

Using the above four equations, we can determine the coordinates representing the intersection numerically with respect to the both coordinate systems as the wave passes by the spherical buoy.

Equilibrium equations

Because the velocities are expressed in the Cartesian coordinates, and the stresses acting on the buoy surface are easier to be manipulated in the moving spherical coordinates, we rotate the stresses τ_{ij} which are now principal with respect to (x, y, z) coordinates

to become τ_{kl} in such a way that τ_{kl} are the principal stresses with respect to $\hat{e}_r$-axis, $\hat{e}_\varphi$-axis, and $\hat{e}_\theta$-axis, where $\hat{e}_r$, $\hat{e}_\varphi$, and $\hat{e}_\theta$ are unit vector bases in the spherical coordinates at time $t = t_i$. Then, we integrate the stresses τ_{kl} over the domain of the intersection at the instant.

Then, the wave loads are

$$W_f = \int_A \tau_{ij} dA = \int_{A'} a_{ki} a_{lj} \tau_{ij} dA' = \int_{A'} \tau_{kl} dA' \tag{34}$$

where, $\tau_{kl} = a_{ki} a_{lj} \tau_{ij}$

$\tau_{ij} = \mu(u_{i,j} + u_{j,i})$: u_i = velosity in i-axis direction

a_{ki}, a_{lj} = direction cosines between $(\hat{e}_r, \hat{e}_\varphi, \hat{e}_\theta)$ and $(\hat{i}, \hat{j}, \hat{k})$

We can calculate now the normal and shear forces due to the weakly viscous wave by integrating the stresses defined above and add the pressure (p) over the intersection as below. The normal force is

$$W_{nf} = \int_\theta \int_\varphi (p + \tau_{rr}) r\cos\varphi d\varphi r d\theta = \int_0^{2\pi} \int_{-\frac{\pi}{2}}^{\varphi} (p + a_{ri} a_{rj} \mu(u_{i,j} + u_{j,i})) r\cos\varphi r d\theta \tag{35}$$

where, $p = \rho\left(\phi_{,t} + \frac{1}{2} u_i u_i\right)$. (36)

There are two components of shear forces acting on the buoy corresponding to the two stress components in the $\hat{e}_\varphi$ and $\hat{e}_\theta$ directions on the sphere. The two shear forces are

$$W_{\theta f} = \int_\theta \int_\varphi \tau_{r\theta} r\cos\varphi d\varphi r d\theta = \int_0^{2\pi} \int_{-\frac{\pi}{2}}^{\varphi} a_{ri} a_{\theta j} \mu(u_{i,j} + u_{j,i}) r\cos\varphi r d\theta \tag{37}$$

$$W_{\varphi f} = \int_\theta \int_\varphi \tau_{r\varphi} r\cos\varphi d\varphi r d\theta = \int_0^{2\pi} \int_{-\frac{\pi}{2}}^{\varphi} a_{ri} a_{\varphi j} \mu(u_{i,j} + u_{j,i}) r\cos\varphi r d\theta \tag{38}$$

According to the Newton' second law, the motion of the buoy on the weakly viscous waves can be described as a equilibrium status among all the forces and moments acting on it. The equilibrium status can be expressed as coupled equations sharing wave loads.

$$\sum_i f_i = M\frac{d^2 z_b}{dt^2} + R_f - W_{vf} = 0 \tag{39}$$

$$\sum_i Mo_i = I\ddot{\varphi} + (\vec{d}_c \times \vec{M}_g - \vec{B}_m - (W_{\theta f}\hat{e}_\theta + W_{\varphi f}\hat{e}_\varphi) \times r\hat{e}_r) \cdot \hat{j} = 0 \tag{40}$$

where, M is the buoy mass, z_b is the vertical location of buoy canter, R_f is the restoring force, W_{vf} is the vertical component of the wave forces, I is the buoy moment of inertia, $\vec{d}_c$ is the location vector connecting from mass center to geometric center of the buoy, $\vec{M}_g$ is the buoy weight, $\vec{B}_m$ is the moment vector by the buoyancy, $W_{\theta f}$, $W_{\varphi f}$ are the shear wave forces, and r is the radius of the spherical buoy. The vertical component in the wave forces is calculated as the inner product of the wave forces expressed in the spherical moving coordinates and the vertical unit vector in the fixed Cartesian coordinates.

$$W_{vf} = (W_{nf}\hat{e}_r + W_{\theta f}\hat{e}_\theta + W_{\varphi f}\hat{e}_\varphi) \cdot \hat{k} \tag{41}$$

The velocity potential and the stream function representing vortical flows are shown in equations (27bc). If the mass center (C_m) is eccentric to geometric center (C_g) of the spherical buoy and the C_m is located below the C_g, then there occurs a restoring moment due to gravity against the exciting moment by shear forces, which causes a oscillating rotational response of the buoy. The coupled equations (39) and (40) are solved numerically. At each time step, the coefficients in the equations are determined corresponding to the instant intersection, and solved through numerical computations. When the C_m is above the C_g, the buoy becomes unstable regarding the rotational response.

Numerical results

Those forces and moments in the above equations are determined at each time step by integrating stresses acting on the instant intersection between the wave and the spherical buoy. The moments in the equation (40) are calculated on the instant vertical position of the buoy at each time step determined by the equation (39). The wave loads causing the buoy responses as exciting force are such that a wave of N wave length long passes by the buoy, which means that the exciting force only exists while the wave intersects with the buoy, and then disappears after it passes away. Water density is set 1. (gr/cm^3), the viscosity is 0.02 ($cm^2 sec$), and the gravity constant is 980. ($cm/sec.^2$). The wavelength and the frequency are 2. (cm) and 73.3 ($rad/sec.$) respectively. The buoy radius is 4**wavelenght*/π, and the buoy material density is set half of the water density. Time step size (dt) is set

Table 1. Dispacements of a spherical buoy and the loads from a weakly viscous wave.

Time (sec)	Vertical Displ. (cm)	Roll angle (Deg.)	Normal force (dyne)	Shear force I (")	Shear force II (")	Shear moment I (dyne*cm)	Shear moment II (")
0.0000	0.00000E+00	0.00000E+00	0.00000E+00	0.00000E+00	0.00000E+00	0.00000E+00	0.00000E+00
0.0054	-1.44406E-06	6.69068E-08	1.42745E+01	5.09852E-02	1.85734E-01	-1.90407E-03	4.67317E-01
0.0108	-4.61265E-05	4.77691E-07	3.81910E+01	9.79153E-02	2.88068E-01	-7.02700E-03	7.13249E-01
0.0162	-2.35436E-04	1.50720E-06	6.41967E+01	1.36786E-01	4.43697E-01	-1.42262E-02	1.08492E+00
0.0215	-6.88570E-04	3.54975E-06	9.61271E+01	1.38762E-01	6.30633E-01	-2.02237E-02	1.52504E+00
0.0269	-1.53191E-03	6.98383E-06	1.23726E+02	1.29068E-01	7.26903E-01	-2.36462E-02	1.72602E+00
0.0323	-2.87961E-03	1.20325E-05	1.49029E+02	8.39897E-02	7.24667E-01	-2.20992E-02	1.67808E+00
0.0377	-4.81093E-03	1.86667E-05	1.51938E+02	1.99252E-02	7.12406E-01	-1.58185E-02	1.60949E+00
0.0431	-7.35010E-03	2.67091E-05	1.40821E+02	-5.52116E-02	5.22816E-01	-6.28400E-03	1.09784E+00
0.0485	-1.04329E-02	3.57820E-05	1.09836E+02	-1.25431E-01	3.77310E-01	4.95549E-03	7.13162E-01
0.0539	-1.39118E-02	4.55046E-05	7.28477E+01	-1.83551E-01	1.06483E-01	1.52597E-02	2.52526E-02
0.0592	-1.76000E-02	5.55431E-05	3.64693E+01	-2.29674E-01	-2.99202E-02	2.53994E-02	-3.03436E-01
0.0646	-2.13016E-02	6.56332E-05	-3.35750E+00	-2.52539E-01	-2.64117E-01	3.20817E-02	-8.76391E-01
0.0700	-2.48144E-02	7.54236E-05	-3.67387E+01	-2.46953E-01	-4.83810E-01	3.70328E-02	-1.39231E+00
0.0754	-2.79495E-02	8.44649E-05	-5.93437E+01	-2.28274E-01	-6.12775E-01	4.20877E-02	-1.66627E+00
0.0808	-3.05618E-02	9.24556E-05	-7.36197E+01	-1.71321E-01	-6.20599E-01	4.35092E-02	-1.63190E+00
0.0862	-3.25578E-02	9.92554E-05	-6.65745E+01	-9.91167E-02	-5.01653E-01	4.36846E-02	-1.27942E+00
0.0916	-3.39084E-02	1.04875E-04	-4.83310E+01	-4.51555E-02	-3.84469E-01	4.10548E-02	-9.44429E-01
0.0969	-3.46632E-02	1.09398E-04	-3.54955E+01	-3.82592E-02	-3.08279E-01	3.82282E-02	-7.19717E-01
0.1023	-3.48789E-02	1.13015E-04	-2.73165E+01	-3.99247E-02	-2.62751E-01	3.66825E-02	-5.77219E-01
0.1077	-3.45895E-02	1.15839E-04	-2.17416E+01	-4.03659E-02	-2.31788E-01	3.54201E-02	-4.76469E-01
0.1131	-3.38220E-02	1.17948E-04	-1.74487E+01	-3.66276E-02	-2.14742E-01	3.49928E-02	-4.04113E-01
0.1185	-3.26016E-02	1.19397E-04	-1.41033E+01	-4.31835E-02	-1.90358E-01	3.44804E-02	-3.27787E-01
0.1239	-3.09547E-02	1.20235E-04	-1.13670E+01	-4.33901E-02	-1.80036E-01	3.42069E-02	-2.73003E-01
0.1293	-2.89097E-02	1.20504E-04	-9.08646E+00	-4.50805E-02	-1.65819E-01	3.40611E-02	-2.22375E-01
0.1346	-2.64976E-02	1.20241E-04	-7.07654E+00	-4.30764E-02	-1.57794E-01	3.30991E-02	-1.75732E-01
0.1400	-2.37522E-02	1.19480E-04	-5.23222E+00	-4.64766E-02	-1.46411E-01	3.25321E-02	-1.33439E-01
0.1454	-2.07101E-02	1.18254E-04	-3.72693E+00	-3.29916E-02	-1.43826E-01	3.05932E-02	-9.73059E-02
0.1508	-1.74104E-02	1.16590E-04	-2.20252E+00	-4.06837E-02	-1.37573E-01	3.00974E-02	-6.24129E-02
0.1562	-1.38952E-02	1.14520E-04	-8.86731E-01	-4.02025E-02	-1.33004E-01	2.89205E-02	-2.80653E-02
0.1616	-1.02081E-02	1.12069E-04	6.72958E-01	-3.23511E-02	-1.31183E-01	2.55203E-02	6.12383E-03
0.1670	-6.39514E-03	1.09266E-04	1.97779E+00	-4.09355E-02	-1.30797E-01	2.45549E-02	3.61671E-02
0.1723	-2.50390E-03	1.06137E-04	3.43455E+00	-3.72892E-02	-1.29199E-01	2.16379E-02	6.87508E-02
0.1777	1.41707E-03	1.02710E-04	4.85796E+00	-3.08794E-02	-1.34876E-01	1.82597E-02	1.03849E-01
0.1831	5.31868E-03	9.90130E-05	6.64701E+00	-3.40419E-02	-1.39916E-01	1.52307E-02	1.40121E-01
0.1885	9.15097E-03	9.50763E-05	8.37009E+00	-3.07831E-02	-1.45842E-01	1.13288E-02	1.79634E-01
0.1939	1.28639E-02	9.09312E-05	1.05435E+01	-3.12635E-02	-1.55346E-01	7.84866E-03	2.21834E-01
0.1993	1.64079E-02	8.66113E-05	1.29058E+01	-2.71048E-02	-1.63342E-01	3.27026E-03	2.68568E-01
0.2047	1.97336E-02	8.21519E-05	1.59946E+01	-3.37583E-02	-1.80429E-01	-1.08199E-03	3.26873E-01
0.2100	2.27917E-02	7.75939E-05	1.98392E+01	-2.48994E-02	-1.93523E-01	-6.69819E-03	3.89184E-01
0.2154	2.55332E-02	7.29794E-05	2.50653E+01	-2.15965E-02	-2.17910E-01	-1.31664E-02	4.69895E-01
0.2208	2.79075E-02	6.83594E-05	3.25367E+01	-2.24465E-02	-2.49396E-01	-1.95831E-02	5.78081E-01
0.2262	2.98609E-02	6.37925E-05	4.46269E+01	-7.66074E-03	-3.02297E-01	-2.87654E-02	7.38313E-01
0.2316	3.13292E-02	5.93629E-05	6.41882E+01	4.13772E-02	-4.06969E-01	-3.78248E-02	1.03907E+00
0.2370	3.22227E-02	5.51948E-05	6.61720E+01	1.13768E-01	-5.09403E-01	-4.55063E-02	1.34015E+00
0.2424	3.24819E-02	5.13183E-05	4.91949E+01	1.63070E-01	-5.46403E-01	-4.76835E-02	1.48124E+00
0.2477	3.21304E-02	4.77623E-05	2.54154E+01	1.98644E-01	-4.66553E-01	-4.47769E-02	1.32919E+00
0.2531	3.12499E-02	4.44728E-05	-6.18016E+00	2.12742E-01	-2.95951E-01	-3.81080E-02	9.35575E-01
0.2585	2.99644E-02	4.13071E-05	-4.12947E+01	1.88799E-01	-7.74356E-02	-2.65531E-02	4.05521E-01
0.2639	2.84312E-02	3.80265E-05	-7.20141E+01	1.54601E-01	6.34920E-02	-1.50762E-02	6.21744E-02
0.2693	2.68042E-02	3.45556E-05	-1.02604E+02	1.06015E-01	3.01305E-01	-4.82034E-03	-5.41606E-01
0.2747	2.52409E-02	3.07653E-05	-1.28618E+02	4.43302E-02	4.90592E-01	3.21179E-03	-1.03974E+00
0.2801	2.38833E-02	2.64801E-05	-1.43422E+02	-2.05533E-02	6.67942E-01	8.25260E-03	-1.51863E+00
0.2854	2.28388E-02	2.14933E-05	-1.39100E+02	-8.05292E-02	6.80605E-01	1.10253E-02	-1.58907E+00
0.2908	2.21421E-02	1.55569E-05	-1.26221E+02	-1.21997E-01	6.10770E-01	1.15961E-02	-1.44897E+00
0.2962	2.17668E-02	8.69400E-06	-1.02468E+02	-1.39883E-01	5.29956E-01	1.03218E-02	-1.27875E+00
0.3016	2.16368E-02	9.88722E-07	-7.17302E+01	-1.30191E-01	4.14232E-01	8.06185E-03	-1.01223E+00
0.3070	2.16355E-02	-7.43535E-06	-3.93795E+01	-1.01192E-01	2.98633E-01	4.99669E-03	-7.40663E-01
0.3124	2.16275E-02	-1.64385E-05	-1.50369E+01	-5.43225E-02	1.67346E-01	1.77334E-03	-4.21987E-01
0.3177	2.14936E-02	-2.57531E-05	-7.35486E-02	-3.37921E-03	-9.15527E-03	1.56241E-05	2.32443E-02
0.3231	2.11456E-02	-3.50683E-05					
0.3285	2.05628E-02	-4.42924E-05					
0.3339	1.97505E-02	-5.34015E-05					
0.3393	1.87169E-02	-6.23700E-05					
0.3447	1.74725E-02	-7.11727E-05					
0.3501	1.60304E-02	-7.97850E-05					
0.3554	1.44057E-02	-8.81826E-05					
0.3608	1.26158E-02	-9.63418E-05					
0.3662	1.06799E-02	-1.04240E-04					

1/50 of the wave period, N is set 1, and the distance between C_m and C_g is set 1/10 of the buoy radius. The shear forces and moments are displayed in Table 1 as well as the vertical displacement and rotation angle. In the figures 3, 4 and 5, we can see how the shear forces and the moments change as time passes. As we find in the table 1, rotational response is quite apparent though with the small moments due to the small shear forces coming mainly from the free surface boundary layer. The shear force I and II in the table and the figures mean the forces acting in the $\hat{e}_\theta$ direction and the $\hat{e}_\varphi$ direction respectively, and the two moments are their corresponding moments about the y - axis, otherwise, do not exist in inviscid flows. The translational and rotational displacements continue to exist for the time being after the wave passes away meaning that the wave loads disappear, and are supposed to die out eventually due to the dissipation mechanism. In Fig. 6 through Fig. 8, an instant intersection and its corresponding force distributions on the buoy surface are displayed when time t = 0.1508 sec. Fig. 6 shows the ϕ coordinates of the wave profile, or how the wave deforms at the instant. The wave profile continues to deform while it passes by the spherical object. The vertical height from the horizontal axis in the Fig. 6 means the vertical displacement of the buoy center at the instant where the origin of the spherical coordinate system is located. Fig. 7 shows the distribution of normal wave force passing as the wave does, and Fig. 8 displays how the shear wave forces work on the buoy surface.

This specific example shows the importance and the role of weakly viscous capillary gravity waves in real water wave problems, and, in addition, the efficiency of multiple coordinate systems corresponding to the orientation of each object. In many cases, for practical and theoretical reasons, the present approach that employs different coordinate systems according to different orientations, may guarantee a promising tool with efficiency and required accuracy.

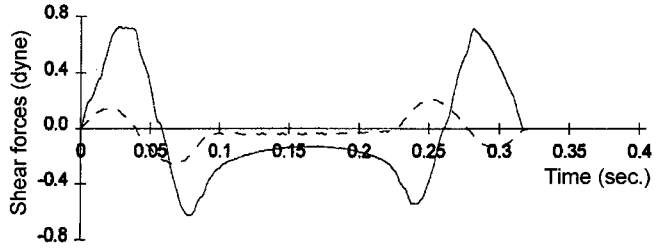

Fig. 3. Shear forces I, II from the viscous wave.

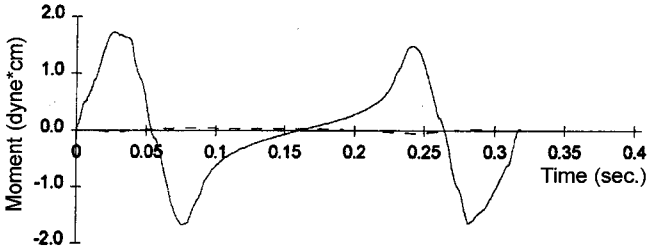

Fig. 4. Moment due to shear force II acting in latitudinal direction.

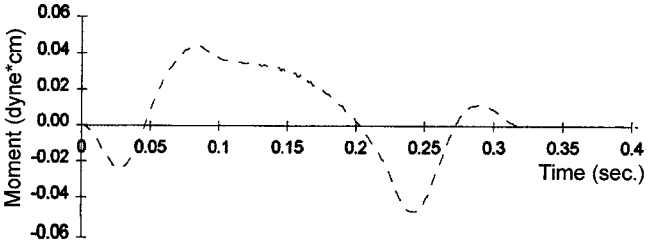

Fig. 5. Moment due to shear force I acting in latitudinal direction.

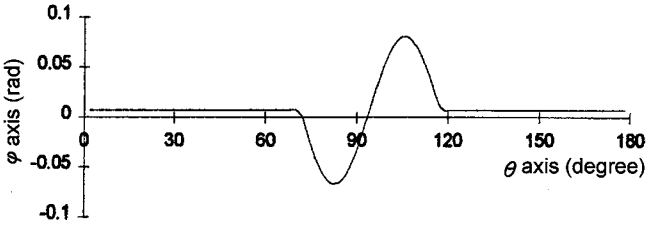

Fig. 6. ϕ coordinate of instant intersection: the wave profile on the buoy surface at t=0.150796 sec.

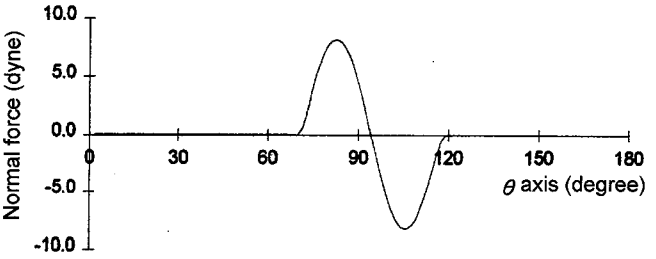

Fig. 7. Normal force distribution on the buoy surface at t=0.150796 sec.

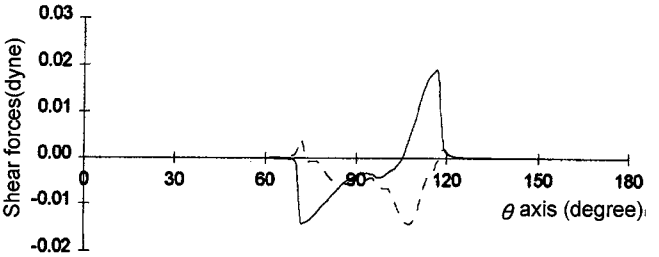

Fig. 8. Shear forces distributions on the buoy surface at t=0.150796 sec.

In this particular problem, the secondary flows due to the existence of the floating object are considered small and ignored as a presumed or well prepared condition.

Viscous waves, surfactants and remote sensing

Ocean surface that covers about two thirds of the Earth, is a boundary region where various oceanic and atmospheric activities occur, which are essential to the Earth's global environment, and their importance are getting bigger as our knowledge or modern technology enhances. Surfactants are the substances which act on the surfaces of bulk fluids. There are so many kinds of surface-active materials, natural or artificial, which cause changes locally and globally in the systems of bulk fluids with surfactants on them. Polluted ocean is a typical example as a by-product of modern industries. Therefore, the understanding of the physics involved in surfactant phenomena becomes a big issue throughout various areas and experts including oceanographers (Journal of Geophysical Research special section, 1992).

Wind waves at seas undergo deformations in the presence of surfactants at their surfaces. It has been asserted that the whole procedure of developing wind waves may be modified due to the changes in the boundary conditions. The damping effect on surface waves due to the existence of surfactants has been explained by modifying the tangential boundary condition regarding viscosity effects and the surface tension. It is usually admitted that surface tension decreases drastically by the presence of surface-active materials (Cini *et al.* 1987).

Marangoni effect

V. Levich introduced the basics of surfactant effects on short viscous water waves in his book (1962). Since then, his approaches and the dispersion relation equation are still in use without big modifications, and many papers have been published by physico-chemists in early years and by the people of geophysics in recent days in accordance with the various trend of modern views.

In late sixties, it was found that, at the surface of a fluid with surfactants, there exists another wave mode in the surface films which is quite different from ordinary water waves though it was hard to be found because it is usually very dissipative and damped out quickly. This newly found wave, which turns out oscillating longitudinally, is considered to be excited by the short viscous waves of bulk fluids vibrating transversely. Since then, the damping effect or the calming effect by surfactants has been understood effectively by the resonance-like interaction phenomenon between the two modes, the longitudinal Marangoni wave and the short viscous Laplace wave. This Marangoni effect depends much on the surfactant dilational properties or the viscosity while the Laplace wave mode relies more on bulk fluid properties (Cini *et al.* 1987 and Lucassen 1982).

On the surface of inviscid fluids, the tangential stress vanishes and normal component balances with the pressure due to the surface curvature by means of Laplace law and uniform surface tension. When surfactants exist, the surface tension is no longer constant and the tangential stress does not vanish either because of the active role of viscosity in the interaction mechanism between the bulk fluids and the surfactants. The periodic contraction and extension of surface, or the periodic horizontal particle velocity change results in periodic deviation of the surface coverage of the surface film from its equilibrium value through a viscous mechanism, which gives rise to a finite tangential stress change varying from point to point at the surface. This viscous mechanism causes changes of surface boundary conditions, more precisely interfacial conditions between surfactants and bulk fluids, induces the periodical longitudinal deformation of surface films , and results in the Marangoni effect through the interaction between those two wave modes as mentioned in the previous paragraph. The Marangoni damping becomes bigger as its wavelength approaches to that of the transverse wave component as resonant phenomenon does, at which the longitudinal motion induces a drastic deviation from the circular orbit motion. Thus there occurs a big change in the fluid motion such as velocity patterns, from irrotational to rotational just beneath the surface film, and vorticity intensity in FSBL flows becomes another active factor that must be taken into account. Therefore, this combined effects cause a big energy dissipation under surface films, which results in calming the fluid surfaces.

In recent years, it was found that the effects by surfactants on ocean surfaces reach more broadly than that of past theories that are directly based on the viscous interaction mechanism mentioned above. In the eighties, a new look on surfactant effects has been issued by H. Hünerfuss and others. It was published by J. Lucassen that the potential increase in damping

is larger in longer waves than the expected amount predicted by the past theory with a proper choice of surface active materials. In other words, not only short ripples but longer capillary-gravity waves were found to be damped out by oil films. The wave attenuation by surface films is attributed to the Marangoni effect that causes a strong resonant-like wave damping in the short wave region, or weakly viscous capillary gravity region. And it is now believed that by means of nonlinear wave-wave interaction phenomenon, wave energy is transferred from longer waves to the energy sink in Marangoni effect wave region, which leads to extra effects on longer waves or the whole wave spectrum (Hünerfuss and Alpers 1989 and Lucassen 1982).

Short waves are also important in remote sensing of sea surfaces. The normalized radar cross section is proportional to the spectral energy density of the wave spectrum according to the Bragg scattering theory. The damped ocean surface can be represented by the relative ratio of the normalized radar cross section between a slick covered surface and a clean surface. The damping coefficient as a function of the wavelength can be obtained by measuring radar back-scatter through varying radar wavelengths and incident angles. The surface roughness at short gravity waves associated with sea slicks has been observed using different measuring methods (JGR special section 1992 and Wismann *et al.* 1993). The observation has shown that radar cross-section decrease and relatively dark images are directly due to the damping of short waves, actually weakly viscous capillary-gravity waves, associated with the concentration of surface microlayer material. Microlayer damping on short waves is caused mainly by the elastic or visco-elastic nature of the thin surfactant layer. The emissivity changes by the presence of surface layers have been also measured.

To observe the damping effect on ocean waves with wavelength of a few meters by monomolecular sea slicks, an experiment was performed by H. Hünerfuss *et al.* in (1989). According to the test results, the damping anticipated by the viscosity effect using past theories was too small and slow to explain the strong and rapid damping of those relatively long waves. Based on their measured data, H.Hünerfuss et al. again mentioned about the unexpected damping in this long wave region confirming that it is due to the combined effects of Marangoni damping on short waves and the nonlinear energy transfer through wave frequencies of different wavelengths in the spectrum.

DISCUSSION

Ocean wave is a typical phenomenon occurring at the upper oceans with various physical factors involved in it such as gravity, water viscosity, surface tension or the interfacial tension between air and sea, the duration of wind blowing, wind direction, wind fetch length, and etc.. Usually, the above factors play more significant roles of their own when the wavelength is short, otherwise some of them become useless, or small enough to be ignored. Most of detailed mechanisms in ocean waves generated by wind start or occur in short waves. For specific and important examples, wind wave generation itself starts due to the interaction between wind and tiny ripples, Marangoni effect mentioned in the last section works on short waves, and electro-magnetic waves used in remote sensing technology interacts far stronger with short capillary or capillary-gravity waves than long waves. Therefore, it becomes more important now than the past to understand the whole and complete nature of short waves. In the past, many of the water wave theories are about inviscid waves, and those theories are advanced enough for their purposes. On the other hand, problems related with viscous waves are comparatively in vague situation. Most of viscous wave problems are investigated by relying upon modification of inviscid results rather than direct approaches to them. Wave breaking also requires better and detailed knowledge in tiny scale hydrodynamics such as the local surface tension changes at deformed wave crests and viscous, rotational or turbulent flows near surfaces (Longuet-Higgins 1992).

In the present paper, a weakly viscous capillary-gravity wave is introduced as an approximation of short real water waves, not a modification of inviscid waves but an approximate solution of a viscous wave equation obtained from the Navier-Stokes equation. Marangoni effect interprets the surfactant damping on waves relying basically on the dispersion equation without any concrete wave forms. All we know about the Marangoni dispersion equation is that it has two roots that represent two wave modes. Therefore, an explicit form of a viscous wave such as WVCG wave introduced in this paper will be handy and needed for direct and clearer investigations into recent viscous wave problems. The detailed trace of spherical buoy motions on a short real wave in the previous section is a direct and concrete application of short

wave theory (Kim and Debnath 1999). Without the WVCG wave, it would not be easy to answer or find out how much the vortical in FSBL work on the buoy motion, which is now simple enough. Polluted ocean environment is another typical example asking various knowledge including oceanographers'.

REFERENCES

Berteaux H.O., 1976. Buoy engineering. John Wiley & Sons, New York, 314 pp.

Cini R., 1987. Ripples Damping Due to Monomolecular Film. *J. Colloid Interface Sci.*, **119**: 74 – 80.

de-Jalon J.G. and Bayo E., 1994. Kinematic and dynamic simulation of multibody system, Springer-Verlag, New York, 440 pp.

Hünerfuss H. and Alpers W., 1989. The Damping of Ocean Waves by Surface Films; A New Look at an Old Problem. *J. Geophys. Res.*, **94**: 6251 – 6265.

Kim N. and Debnath L., 2000. Motion of a buoy on a weakly viscous capillary gravity waves. *Int. J. Non-Linear Mech.*, **35**: 405 – 420.

Kim N. and Debnath L., 1999. Resonance wave interactions in a weakly viscous liquid. *Int. J. Non-Linear Mech.*, **34**: 197 – 220.

Levich V. G., 1962. Physicochemical hydrodynamics. Prentice Hall, New Jersey, 700 pp.

Longuet-Higgins M. S., 1992. Capillary rollers and bores. *J. Fluid Mech.*, **240**: 659 – 679 pp.

Lucassen J., 1982. Effect of Surface-Active Material on the Damping of Gravity Waves: A Reappraisal. *J. Colloid Interface Sci.*, **85**: 52 – 58.

McLaughlin J. B., 1991. Inertial migration of a small sphere in linear shear flows. *J. Fluid. Mech.*, **224**: 261 – 274.

Miles J.W., 1990. Capillary-viscous forcing of surface waves. *J. Fluid Mech.*, **219**: 635 – 646.

Rusanov A. I. and Prokhorov V. A., 1996. Interfacial Tensionmetry. Elsevier Science, Amsterdam, 407 pp.

Schlichting H., 1979. Boundary-Layer Theory. McGraw-Hill, New York, 817 pp.

Wismann V., Theis R., Alpers W. and Huenerfuss H., 1993. The damping of short gravity-capillary waves by experimental sea slicks measured by an airborne multi-frequency microwave scatterometer. *IEEE.*, **93**: 342 – 347 pp.

Whitham G. B., 1974. Linear and nonlinear waves. John Wiley & Sons, New York, 636 pp.

Special Section: Sea Surface Microlayer, 1992. *J. Geophys. Res.*, **97**: 5201 – 5330 pp.

Manuscript received September 22, 1999
Revision accepted December 22, 1999
Editorial Handling: Sang-Ho Lee